

Electronic Supplementary Information for:

Temperature Controlled Invertible Selectivity of Adsorption of N₂ and CH₄ by Molecular Trapdoor Chabazites

Jin Shang,^{*a,b} Gang Li,^c Qinfen Gu,^d Ranjeet Singh,^{a,b} Penny Xiao,^{a,b} Jefferson Z. Liu,^{*e} and Paul A. Webley^{*a,b}

^a Cooperative Research Center for Greenhouse Gas Technologies (CO2CRC), Melbourne, Australia

^b Department of Chemical and Biomolecular Engineering, The University of Melbourne, Victoria 3010, Australia. E-mail: paul.webley@unimelb.edu.au

^c Centre for Energy, School of Mechanical and Chemical Engineering, The University of Western Australia, Crawley WA 6009, Australia

^d Australian Synchrotron, 800 Blackburn Rd, Clayton, Victoria 3168, Australia

^e Department of Mechanical and Aerospace Engineering, Monash University, Clayton, Victoria 3800, Australia. E-mail: zhe.liu@monash.edu

Index

S1. Schematic Representation of Chabazite Structure and Cation Positions

S2. Computational Set Up for Density Functional Theory (DFT) Calculations

S3. Site Preference for K cation in r2KCHA

S4. *In Situ* Synchrotron PXRD of Adsorption Experiments

S5. Binding Energies for N₂ and CH₄ on r2KCHA Calculated by DFT

S6. References

S1. Schematic Representation of Chabazite Structure and Cation Positions



Fig. S1 Schematic representation of chabazite structure and cation positions. Double-six ring prisms (D6Rs) connected by tilted four-membered rings (4MRs) form a three-dimensional structure creating eight-membered rings (8MRs) as the only access to the crystal interior. Four cation sites exist: inside the center of a D6R (SI); inside the supercavity above a D6R (SII); inside the supercavity next to a 4MR (SIII); in the center of an 8MR (SIII').

S2. Computational Set Up for Density Functional Theory (DFT) Calculations

All results were calculated using the Vienna *Ab initio* Simulation Package (VASP)¹ with the projector augmented waves (PAW) approach.² The cut-off energy of the plane wave basis-set was 405 eV. A gamma point only *k*-point mesh was used for one unit cell of chabazite (including three double six-ring prisms or one and a half supercavities). Such cut-off energy and *k*-point mesh have been tested to ensure the total energy value convergence within 1 meV/atom. The atomic positions were optimized with the conjugate gradient method until the forces acting on atoms were below 0.015 eV/Å, as suggested by Gödl and Hafner.³ To take account of the van der Waals interactions in our material systems, we have adopted optB86b.⁴⁻⁶

We applied the climbing image nudged-elastic-band (CI-NEB) method for energy barrier calculations.

S3. Site Preference for K cation in r2KCHA

DFT calculations show that the total energy of a potassium chabazite with one K at the 8MR doorway (site SIII') is the lowest followed by site SII, suggesting site SIII' is the most preferred position and site SII is the second preferred position.

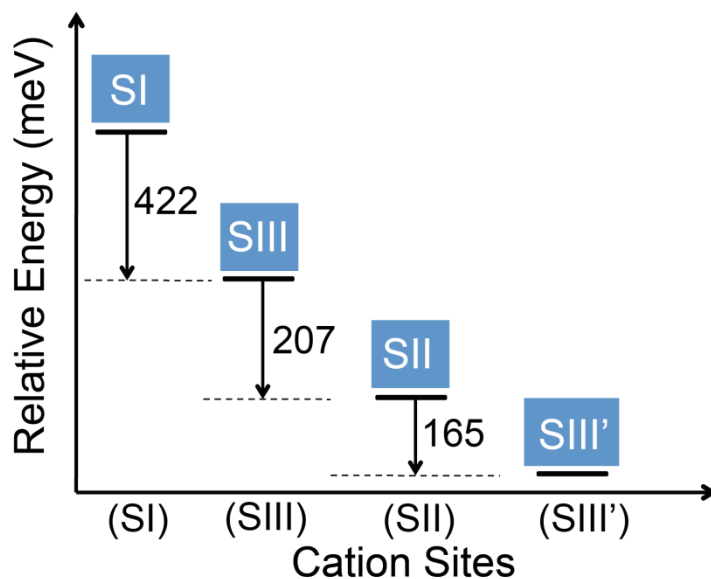


Fig. S2 Relative total energy of a potassium chabazite with one K cation at different sites. Site SIII' associates with the lowest total energy, representing the most stable cation site for K.

S4. In Situ Synchrotron PXRD of Adsorption Experiments

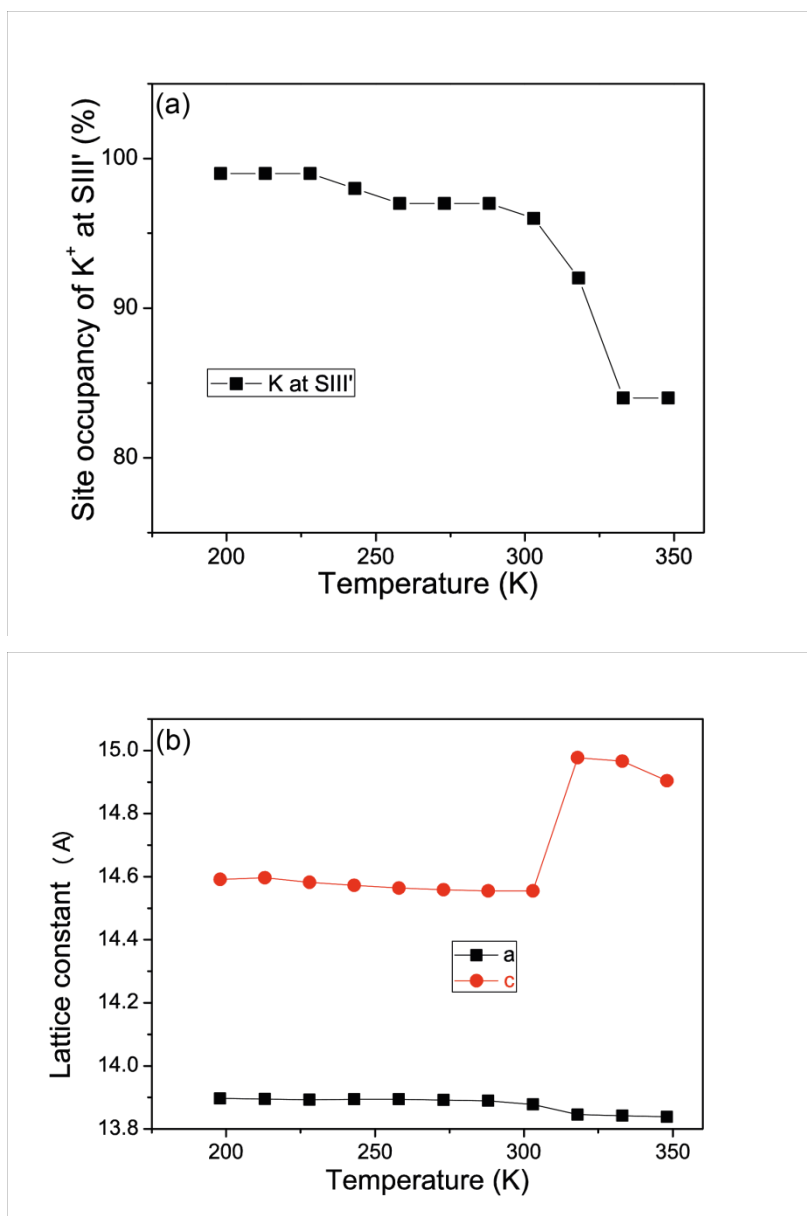


Fig. S3 Evolution of K^+ occupancy at $SIII'$ and lattice constant with temperature. (a) Above 303-313 K, $SIII'$ site occupancy reduces from 100%, leading to the opening of pore apertures. (b) Above 303 K, lattice constant a starts to decline and c to incline indicating cation migration. The estimated error in site occupancy is 3% and in lattice constant is 0.2%. Lines are guides to the eye.

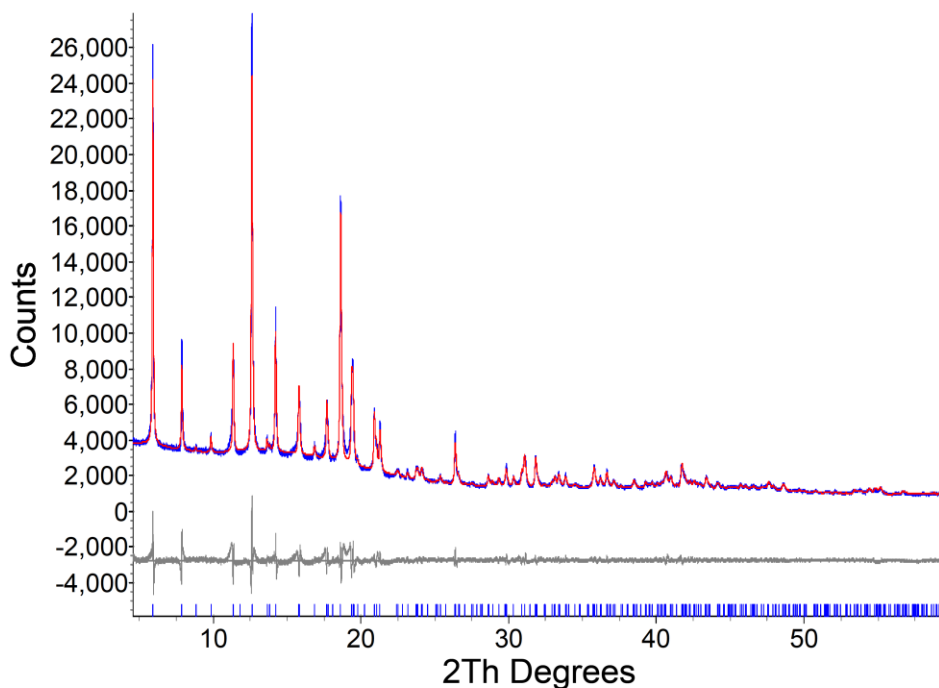


Fig. S4 Rietveld refinement profile for chabazite (**r2KCHA**) phase under CO₂ atmosphere at 303 K. Observed (blue), calculated (red), difference (grey) plots. The refined agreement factors are $R_{wp} = 5.5\%$, $R_B = 4.9\%$ and $GoF = 2.16$. $\lambda = 0.9535 \text{ \AA}$. Note that the temperature at which cation occupancy substantially changes (denoting cation migration) is independent of the atmospheres as verified in the case of **r2CsCHA**;⁷ therefore we reasonably employed the synchrotron data under CO₂ to study the temperature dependence of cation occupancy in **r2KCHA**.

Table S1. Summary of experiment and crystallographic details for chabazite (**r2KCHA**) phase (rhombohedral setting) under CO₂ at 303K.

Parameters	values
Formula sum	Si _{3.72} Al _{8.28} O ₂₄ K _{3.6}
Formula weight	852.624 g/mol
Crystal system	trigonal
Space-group	R-3 m (166)
Cell parameters	$a = 9.3588(2) \text{ \AA}$, $\alpha = 95.6337(15)^\circ$
Cell volume	$806.98(6) \text{ \AA}^3$
Z	1
Calc. density	1.75437 g/cm^3
2theta, deg	$2\theta \text{ min} = 4$, $2\theta \text{ max} = 84$

Detector	Mythen-II, Australian Synchrotron
Wavelength	0.9535 Å
R_B	4.9 %
R_{wp}	5.5 %
GoF	2.16

Table S2. Atomic coordinates following refinement of chabazite (**r2KCHA**) under CO₂ at 393K.

Atom	Wyck. site	S.O.F.	x/a	y/b	z/c
Si	12i	0.31	0.1004(6)	0.3333(3)	0.8780(7)
Al	12i	0.69	0.1004(6)	0.3333(3)	0.8780(7)
O1	6f	1	0.2443(5)	-0.2443(5)	0
O2	6g	1	0.1182(3)	-0.1182(3)	½
O3	6h	1	0.2930(8)	0.2930(8)	0.8831(4)
O4	6h	1	0.0315(6)	0.0315 (6)	0.3118(9)
K1	3e	0.96	0	½	½
K2	2c	0.36	0.2388(13)	0.2388(13)	0.2388(13)

S5. Binding Energies for N₂ and CH₄ on r2KCHA Calculated by DFT

In our *ab initio* simulations, the K form chabazite with Si/Al ratio of 3 (**r3KCHA**) was constructed to represent a typical high cation density chabazite (nine cations per unit cell);⁸ To study the interactions between the chabazite and the guest gas molecules, a single gas molecule was placed close to the K⁺ cations (one gas molecule per unit cell), and then the complex was fully relaxed *via* the conjugate gradient algorithm. The adsorption energy (calculated at 0 K) of different guest gas molecules is defined as the difference between the total energy of the chabazite–gas molecule adsorption complex and the total energy of chabazite (CHA) augmented by the energy of the isolated single gas molecule:

$$E_{\text{ads}} = E_{\text{tot}}(\text{CHA}+\text{gas}) - E_{\text{tot}}(\text{CHA}) - E_{\text{tot}}(\text{gas}).$$

S6. References

1. G. Kresse and J. Furthmüller, *Phys. Rev. B*, 1996, **54**, 11169-11186.
2. G. Kresse and D. Joubert, *Phys. Rev. B*, 1999, **59**, 1758-1775.
3. F. Göltl and J. Hafner, *J. Chem. Phys.*, 2011, **134**, 0641021-06410211.
4. J. Klimeš, D. R. Bowler and A. Michaelides, *Phys. Rev. B*, 2011, **83**, 195131.
5. J. Klimeš, D. R. Bowler and A. Michaelides, *J. Phys.: Condens. Matter*, 2010, **22**, 022201.

6. K. Lee, É. D. Murray, L. Kong, B. I. Lundqvist and D. C. Langreth, *Phys. Rev. B*, 2010, **82**, 081101.
7. J. Shang, G. Li, R. Singh, Q. Gu, K. M. Nairn, T. J. Bastow, N. Medhekar, C. M. Doherty, A. J. Hill, J. Z. Liu and P. A. Webley, *J. Am. Chem. Soc.*, 2012, **134**, 19246-19253.
8. J. Shang, G. Li, R. Singh, P. Xiao, J. Z. Liu and P. A. Webley, *The Journal of Physical Chemistry C*, 2013, **117**, 12841-12847.